Pergamon

Bioorganic & Medicinal Chemistry, Vol. 5, No. 3, pp 535–547, 1997

PII: S0968-0896(96)00267-2
0968-0896/97 $17.00 + 0.00

Possible Ligand–Receptor Interactions for NK_1 Antagonists as Observed in their Crystal Structures

Gertjan J. Boks,[a,*] Jan P. Tollenaere[a] and Jan Kroon[b]

[a]*Department of Medicinal Chemistry, Utrecht Institute for Pharmaceutical Sciences, Universiteit Utrecht, Sorbonnelaan 16, NL-3584 CA Utrecht, The Netherlands*

[b]*Department of Crystal and Structural Chemistry, Bijvoet Centre for Biomolecular Research, Universiteit Utrecht, Padualaan 8, NL-3584 CH Utrecht, The Netherlands*

Abstract—Crystal structures of nine non-peptide tachykinin NK_1 antagonists have been analysed for the intermolecular interactions of their pharmacophoric groups with neighbouring molecules in the crystals. Experimental data on interaction geometries of these antagonists with their environment can be of help in understanding the mechanism of binding to the human NK_1 receptor. Several interaction geometries have been identified that are consistent with both structure–activity relationships and reported receptor interactions for the compounds analysed. In addition, an interaction site for the side-chain of Gln-165 in the human NK_1 receptor that is probably involved in donating a hydrogen bond to the benzylamino nitrogen or benzylether oxygen of the quinuclidine and piperidine antagonists is explicitly postulated. Also, a superposition based on pharmacophoric elements in the crystal structure conformations of two prototypic NK_1 antagonists, CP-96,345 (**1**) and CP-99,994 (**4**), suggests how both compounds might interact with the human NK_1 receptor in a similar manner.

Introduction

Crystal structures have an established role in providing us with energetically accessible conformations of bioactive compounds and thereby providing a basis for structure-based ligand design.[1] However, one usually relies on information from secondary sources such as crystal structure statistics and theoretical studies on model systems for locating the possible intermolecular interactions of these compounds. The information on interactions enclosed in the crystal structures of the compounds itself is, however, scarcely used, although it may well reflect interactions with a macromolecular receptor.[1,2] Both in ligand–receptor binding as in crystallization a compromise is achieved between lowering the conformational energy and maximizing the number of intermolecular interactions. The underlying physical principles to both processes are the same and it is therefore likely that similar interaction geometries can be present both in the solid crystalline state of a ligand and when bound to a receptor. A detailed study of the crystal structures of nine tachykinin NK_1 antagonists was performed to document the experimentally observed interactions with their crystal environment. These interactions were then compared to the compounds' structure–activity relationships, knowledge of the bioactive conformation and results from receptor mutagenesis studies that have been reported for some of these ligands.[3]

Non-peptide NK_1 antagonists are of interest, because of their potential anti-inflammatory and antinociceptive action. A possible role has been proposed for NK_1 antagonists in the relief of chronic pain and in the treatment of tachykinin-mediated bronchoconstriction and plasma extravasation in asthma.[4] A dipeptide-based NK_1 antagonist, FK888, has already entered clinical trials for the treatment of asthma.[5] In addition, a potent anti-emetic NK_1 antagonist with good bioavailability was recently reported.[6] It might be valuable in the control of emesis (vomiting) resulting from, for example, chemotherapy. Detailed knowledge of the interaction mechanism of antagonists with the NK_1 receptor is of importance for the development of selective pharmacological tools for further unravelling the role of tachykinins in a number of these pathophysiological processes, which can open perspectives for the development of new drugs. In these efforts, our results can be used in the construction of binding-site or receptor models for these antagonists, in the absence of an experimental structure of the NK_1 receptor.

A generalized (non-peptide) NK_1 antagonist pharmacophore is shown in Figure 1(a). This pharmacophore merely reflects the requirement of two aromatic rings for high-affinity NK_1 antagonism, kept in the proper spatial arrangement by a great variety of possible scaffolds.[5] A variety of scaffolds is present in the compounds included in this study (Fig. 2). They represent four different chemical classes of NK_1

*Gertjan J. Boks, Department of Medicinal Chemistry, Universiteit Utrecht, Sorbonnelaan 16, NL-3584 CA Utrecht, The Netherlands; telephone: +31 30 253 6958/6979; fax: +31 30 253 6655; e-mail: G.J.Boks@far.ruu.nl
Key words: NK_1 antagonists, crystal structures, intermolecular interactions, ligand–receptor interactions.

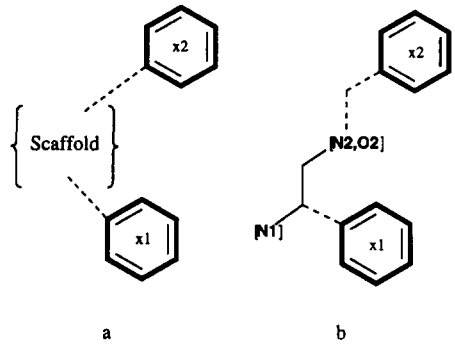

Figure 1. (a) Generalized non-peptide NK_1 antagonist pharmacophore consisting of two (or more) aromatic rings held together by various scaffolds. (b) A more detailed NK_1 non-peptide antagonist pharmacophore based on previously reported pharmacophoric elements for quinuclidine and piperidine NK_1 antagonists. Pharmacophoric elements are indicated in bold.

Table 1. Binding affinities for the human NK_1 receptor determined in various assays

No.	Name	IC_{50} (nM)	Reference
1	CP-96,345	0.66 ± 0.26	14
2		12.2 ± 2.9	27
3	L-709,210	0.2	12
4	CP-99,994	0.17 ± 0.04	16
5	CP-210,053	2[a]	23
6	CP-211,754	0.61 ± 0.058	10
7	L-708,568	67 ± 10	26
8	L-732,244	22 ± 7	11
9		0.34±0.07	17

[a]Determined as the racemate.

antagonists: quinuclidines (**1–3**), piperidines (**4–6**), L-tryptophan benzyl esters (**7** and **8**), and isoquinolineurea and pyrido[3,4-*b*]pyridine carboxamide (**9**) derivatives. All compounds have high-affinity (IC_{50} < 15 nM) or medium affinity (IC_{50} 15–150 nM in our definition) for the human NK_1 receptor (Table 1). A common part of the quinuclidine and piperidine scaffolds is exemplified by a 1,2-disubstituted ethane fragment connecting the two pharmacophoric heteroatoms[7] as shown in Figures 1(b) and 3. This structural element can tentatively also be recognized in compounds **7** and **9** (Fig. 4). Although a different detailed mechanism of interaction with the NK_1 receptor can be expected, a similar structural role for the scaffolds is hypothesized as is, for instance, indicated by the common receptor binding sites for the L-tryptophan benzylester **7** and the benzylether quinuclidine **3**.[8] With the aid of the crystal structure data of these compounds we were able to suggest interaction geometries between these compounds and Gln-165, His-197, Phe-268, Tyr-272 and His-265 in the human NK_1 receptor.

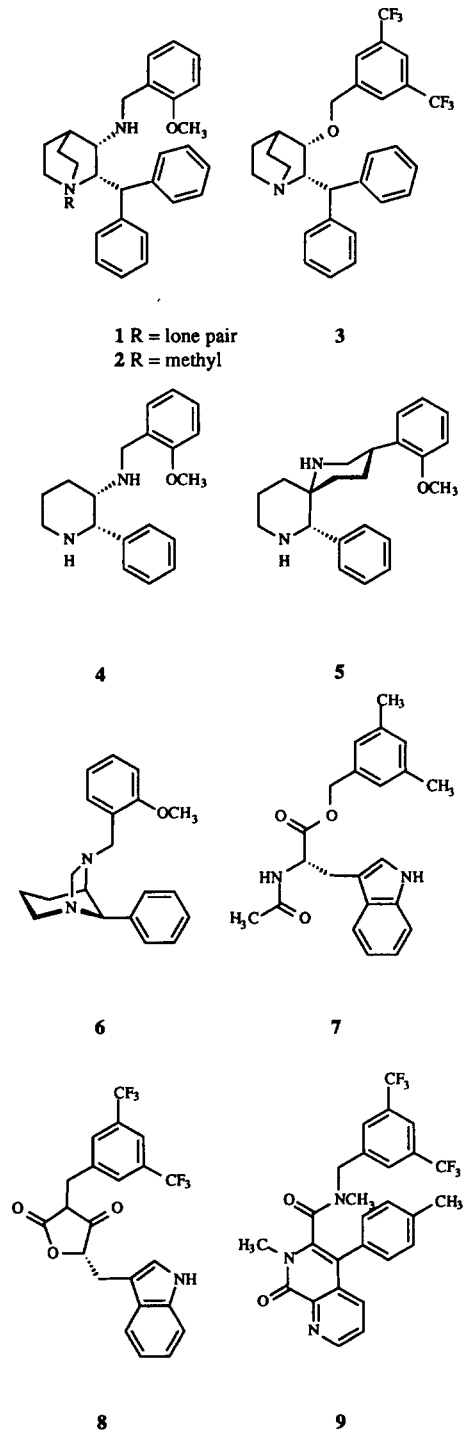

Figure 2. Structural formulas of the non-peptide NK_1 antagonists included in this study.

Methods and Materials

Crystal structures

The crystal data and atomic coordinates were either taken from the supplementary material of the corresponding reports or from the Cambridge Structural Database (CSD).[9] The crystal data for compound **6**, CP-211,754 were kindly provided by Dr H. R. Howard.[10] Data for compounds **3** and **8** were kindly provided by Dr R. T. Lewis and Dr R. G. Ball.[11,12] In cases where atomic positions for hydrogens were absent, they were calculated using the CRYSIN module of the SYBYL package (Version 6.2).[13] A summary of selected crystallographic data for the set of antagonists analyzed is presented in Table 2. Five compounds were co-crystal-

Table 2. Selected crystallographic data for the NK_1 antagonists analyzed

No.	Name	Formula	Space group	*R*-factor[a]	CSD Refcode and reference
1a	CP-96,345 free base	$C_{28}H_{32}N_2O$	P-1	0.040	YAFJOE, 14
1b	CP-96,345 dimesylate salt	$C_{28}H_{32}N_2O{\cdot}2CH_3SO_3H$	P-1	0.123[b]	YAFJUK, 14
2	*N*-methyl analogue of CP-96,345[c]	$[C_{29}H_{35}N_2O^+][I^-]$	$P2_1$	0.072	LEWCUL, 17
3	L-709,210 hydrochloride[d]	$C_{29}H_{27}NOF_6{\cdot}HCl$	P-1	0.096	12[e]
4	CP-99,994 dihydrochloride[f]	$C_{19}H_{24}N_2O{\cdot}2HCl{\cdot}0.05CH_3OH$	$P2_1/n$	0.055	LACPOU, 16
5	CP-210,053 dihydrochloride[g]	$C_{22}H_{28}N_2O{\cdot}2HCl{\cdot}H_2O$	Pbca	0.0603	YICLEB, 23
6	CP-211,754	$C_{20}H_{24}N_2O$	$P2_1$	0.0348	10, Courtesy of H. R. Howard[e,h]
7	L-708,568	$C_{22}H_{24}N_2O_3$	$P2_1$	0.045	26
8	Inactive enantiomer of L-732,244[d]	$C_{21}H_{14}N_2O_3F_6$	$P2_12_12_1$	0.057	11, Courtesy of R. T. Lewis, R. G. Ball[e,h]
9		$C_{27}H_{21}N_3O_2F_6$	$P2_1/n$	0.096	17

[a]*R*-factor $=\Sigma||F_o|-|F_c||/\Sigma|F_o|$, in which $|F_o|$ and $|F_c|$ are the moduli of the observed and calculated structure factors, respectively.
[b]The authors report that this relatively high *R*-factor is likely to be due to the low quality of the crystal related to its sensitivity to the atmosphere.
[c]The antagonist carries a permanent positive charge; it has been crystallized as the monoiodide salt.
[d]The trifluoromethyl groups were rotationally disordered and modelled over two sets of staggered conformations.
[e]This structure will be available in future releases of the Cambridge Structural Database (CSD).
[f]The methanol was found to be disordered with an occupancy of 0.05. Hydrogen positions on methanol were not located.
[g]Hydrogen positions on the water molecule were disordered.
[h]Personal communication.

lized with other small molecules (**1b–5**), either counterions, water or methanol. Compound **1** (CP-96,345) is present in two crystal forms: the free base (**1a**) and as the dimesylate salt (**1b**). The protonation state of CP-96,345 in **1b** was not reported.[14] However, the stoichiometry of the crystal, the basicity of the nitrogen atoms, the acidity of the methanesulfonic acid together with the resulting hydrogen bond network revealed that both amine nitrogens in **1b** are protonated. The protonation state of the other compounds as reported for these crystal structures was confirmed by our analyses. Six crystal structures are encountered in centrosymmetric space groups. For the chiral compounds (**1a**, **1b**, **3**, **4** and **5**) this implies that they have been crystallized as racemic mixtures of two enantiomers. This should be kept in mind in relation to the pronounced stereoselectivity of some of these compounds.[12,15,16] Compound **9** is achiral, which in view of the centrosymmetric space group implies that two conformations of the same molecule, which are mirror images of one another, are present in the crystal structure.[17] For compound **8** only the crystal structure of the inactive *R* enantiomer was available to us,[11] but inversion of the complete crystal structure is allowed without compromising the integrity of the X-ray diffraction experiment. A general error check on all structures was performed using PLATON.[18]

Evaluation of interactions

In the analysis of intermolecular contacts, molecules/groups in van der Waals contact or at least surrounding the active stereoisomer in the crystal structures have been identified using the SYBYL package.[13] Molecules were considered to be 'in van der Waals contact' or 'surrounding' if in any pair of non-hydrogen atoms, not belonging to the same molecule, the atoms were no more than 5 Å apart. Intermolecular contacts for functional groups that are considered to be important for the activity of the compounds were classified and geometrically evaluated in terms of documented intermolecular interactions (see e.g. Burley and Petsko[19]). For details on the determination of interaction geometries see Experimental.

Hydrogen bond analyses of all structures in their established protonation state, and with their crystallographically determined hydrogen positions, were performed with PLATON.[18] For the evaluation of possible C–H...X interactions,[20] X being N, O, or Cl and I (usually as anions), hydrogen bond criteria were applied (see Experimental). For this analysis corrected hydrogen positions in the structures have been calculated using the CRYSIN module of the SYBYL package. These new hydrogen positions result from the normalization of bond lengths involving hydrogen atoms; the values determined by X-ray crystallography are systematically shorter by about 0.1 Å than their actual values, which can be determined by neutron diffraction.[21] Additionally, all C–H groups not considered as being involved in C–H...X interactions, but with hydrogen atoms within van der Waals radius of any possible acceptor atom were identified. This facilitated the localization of possible patterns of C–H...X contacts, which might be more informative than restricting oneself to the interactions revealed by strictly applying the hydrogen bond criteria.[22]

In the course of the study the need was felt to include molecular models of the NMR conformation[23] of compound **5** and the nitrogen N2 inverted configuration of compound **6** for comparison to the crystal structure conformations. A combination of molecular dynamics simulations followed by semi-empirical geometry optimizations using the AM1 Hamiltonian[24] in the MOPAC93 program[25] provided these models. See Experimental for details. Calculations were performed on Silicon Graphics INDY and Crimson Elan workstations.

Results

The crystal structure conformations of the quinuclidine and piperidine antagonists are depicted in Figure 3. The

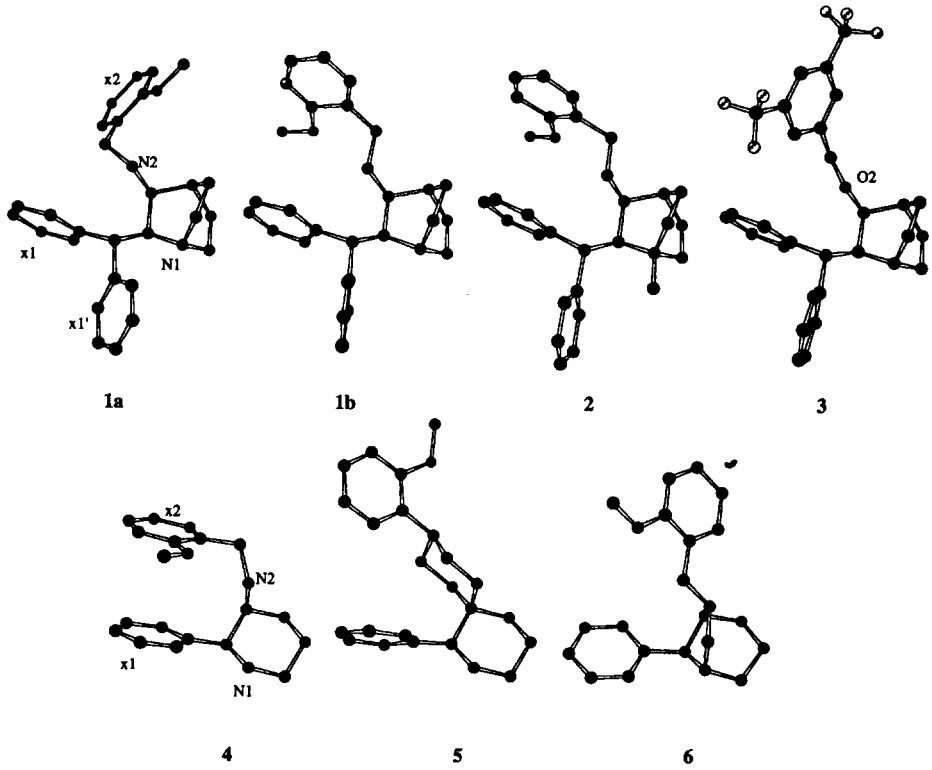

Figure 3. Crystal structure conformations of the quinuclidine (upper row) and piperidine (bottom row) antagonists. Atom labelling of pharmacophoric groups and selected atoms is indicated for representative compounds in each row. x1, x1′ and x2 are used to indicate both the aromatic ring itself as well as the rings' centroid.

crystal structure conformations of compounds 7,[26] **8** and **9** are depicted in Figure 4. The assignment of aromatic ring centroids x1 and x1′ in structures **1a**, **1b**, **2**,[27] **3** and **9** (Figs 3 and 4) is based on the mutual correspondence of the x1–x2 and x1′–x2 distances in these structures (data not shown) and the correspondence of the x1–x2 distance of CP-96,345 (**1a** and **1b**) with that of CP-99,994 (**4**) in molecular modelling studies as described by Desai et al.[16]

Intermolecular interactions encountered in the crystal structures are (charge-assisted) hydrogen bonds and charged nitrogen–aromatic interactions for N1 and N2, C–H...X interactions (X being O, chloride, or iodide) for carbon atoms adjacent to a positively charged nitrogen atom and aromatic–aromatic stackings and hydrophobic interactions for the aromatic groups in the molecules. Below we describe these interactions and their interaction geometries in more detail, with an emphasis on the interactions of the pharmacophoric groups.

Quinuclidine antagonists

Whenever the quinuclidine nitrogen N1 is positively charged (**1b**, **2** and **3**) there are always two anions present at similar positions in space. These positions are indicated as I and II in Figure 5. These anion positions might mimic the positions of hydrogen bond acceptor groups or anionic groups in the NK_1 receptor. The anion positions as given in Table 3 are defined relative to the quinuclidine rings. In Figure 5, the interaction geometry in structure **3** is used as an example. When the positive charge of N1 is due to protonation, the anion in

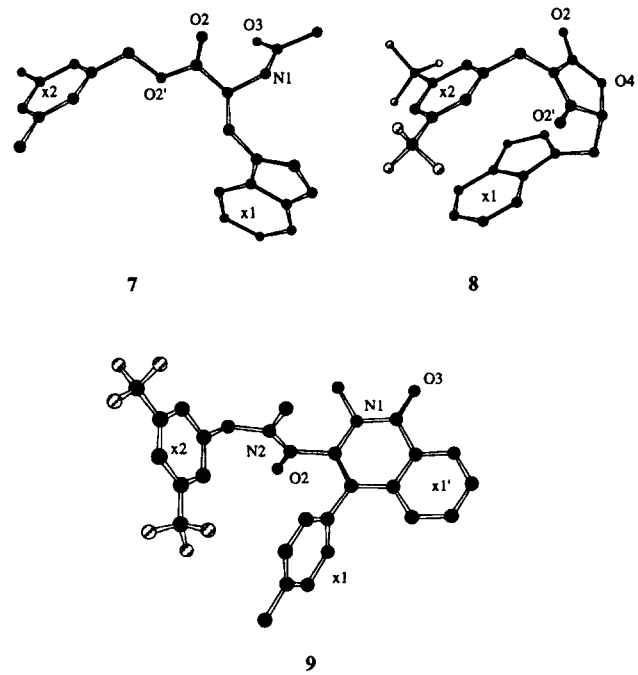

Figure 4. Crystal structure conformations of the L-tryptophanbenzyl ester (upper row) and pyrido[3,4-*b*]pyridine carboxamide (bottom row) antagonists. For compound **8** the crystal structure conformation of the inactive *R* enantiomer is depicted. For compound **9** only one of the two mirror image conformations present in the structure is shown. Atom labelling of pharmacophoric groups is indicated for representative compounds in each row.

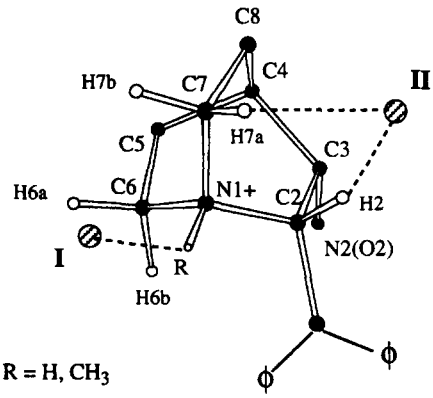

Figure 5. Common anionic interaction sites for quinuclidine NK_1 antagonists. The structure of L-709,210 (**3**) serves as an example.

position I is bonded by a charge-assisted hydrogen bond with N1. In structure **2** the iodide anion in position I is stabilized by a C–H...I^- interaction from the methyl group attached to N1. In position II the anion positions are stabilized by C–H...X interactions arising from either C2–H (**2**) alone or both C2–H and C7–H (**1b** and **3**) (Fig. 5). The similarity in anion positions is reflected in the dihedral angles N1–C2–C3–Ac for positions I and II as given in Table 3. In the only structure with a neutral quinuclidine nitrogen (**1a**), positions I and II are occupied by phenyl rings.

In addition to the anions, the quinuclidine rings carrying a positively charged N1 nitrogen are surrounded by phenyl rings stabilized by charged nitrogen–aromatic interactions.[28,29] These phenyl rings are all positioned on one hemisphere of the quinuclidine ring, as can be seen in the superposition in Figure 6, but not all positions occupied are equivalent. There are positions exclusively occupied by aromatic rings while others are also occasionally occupied by anions in other

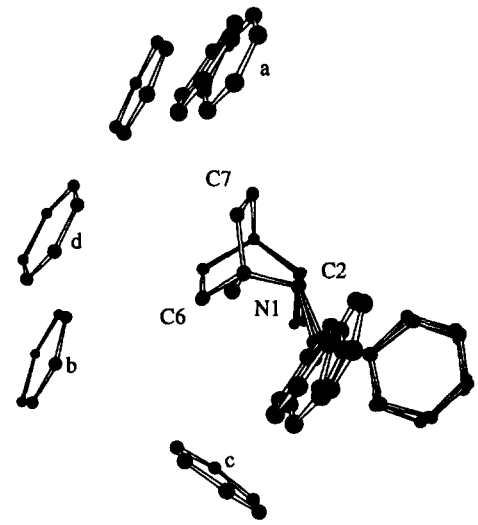

Figure 6. Charged nitrogen–aromatic interaction geometries as observed around the positively charged quinuclidine rings. The quinuclidine rings have been superimposed. The substituted benzyl groups have been omitted for clarity.

structures. Interaction geometries are given in Table 4. Position *a*, above C7 in Figure 6, is occupied by a phenyl ring in three structures (**1b**, **2** and **3**) and the ring is tilted from a perpendicular position towards the vector N1–C7. However, this position is also occupied by a phenyl ring in the crystal structure of the neutral quinuclidine (**1a**). Position *d* is occupied by a phenyl ring in structure **3** and by a mesylate anion in structure **1b**, both making van der Waals contact with the quinuclidine ring. The phenyl ring position designated *c* (structure **2**) is stabilized by both charged nitrogen–aromatic interactions and C–H...π interactions donated by the benzhydryl group.

Table 3. Common intermolecular hydrogen bond acceptor/C-H...X contact acceptor groups surrounding quinuclidine antagonists[a]

			Position I			
No.	**Donor**	**Acceptor[b]**	**N1...Ac (Å)[c]**	**C2-N1...Ac (°)**	**C2-N1-R-Ac[d] (°)**	**N1-C2-C3-Ac (°)**
1b	N1-H	O(5) mesylate	2.686(19)	130.7	−176.5	−7.2
	C6-H6a	O(7) mesylate	3.91(2)	153.6	−155.5	−18.1
2	C1-H[e]	I(1) iodide	4.652	165.5	−172.7	−6.8
3	N1-H	Cl(1) chloride	3.113(5)	136.0	152.0	8.4

			Position II			
No.	**Donor**	**Acceptor**	**N1...Ac (Å)**	**N1-D...Ac (°)**	**N1-D-H-Ac (°)**	**N1-C2-C3-Ac (°)**
1b	C2-H2	O(6)′ mesylate	3.97(2)	101.1	−15.8	108.7
	C7-H7a	O(5)′ mesylate	4.21(2)	116.4	167.5	76.1
2	C2-H2	I(1)′ iodide	4.845	111.0	−109.3	113.2
3	C2-H2	Cl(1)′ chloride	4.107(5)	91.8	−8.8	98.9
	C7-H7a	Cl(1)′ chloride	4.107(5)	99.4	68.6	98.9

[a]Atom labelling as given in Figure 5. Ac and D are the general notation for an acceptor group and a donor carbon atom, respectively. The table has been constructed in such a way that reconstruction of the anion positions relative to the antagonist structures is possible.
[b]The acceptor atoms are indicated with the atom labelling from the original publication, as given in parentheses. A prime indicates a position related by crystallographic symmetry to the acceptor atom mentioned in the table previously.
[c]Values in parentheses are estimated standard deviations (esds) in the last digit. For compound **2** no esds were available to us.
[d]R is either the N1 attached hydrogen or the C1 carbon of the methyl group attached to N1 in compound **2**.
[e]C1 is the carbon atom of the methyl group attached to N1.

Table 4. Observed charged nitrogen–aromatic interaction geometries for quinuclidine antagonists in their crystal structures[a]

No.	C(N1+)	Position in Figure 6	Interaction geometry[b]	N1...x (Å)	C(N1+)...x (Å)	θ (°)	φ (°)	C2-N1-C(N1+)...x (°)
1b	C7	a	2	5.618	4.258	20.5	46.4	−123.4
2	C7	a	2	5.417	4.057	22.3	36.7	154.4
	C6	b	2	5.993	4.543	16.8	55.8	162.0
	C6	c	1	5.292	4.749	61.3	29.2	72.5
	C1	c	1	5.292	5.032	71.9	29.2	−75.4
3	C7	a	2	5.650	4.251	18.3	53.6	−101.3
	C7	d	1	5.268	5.015	72.1	35.7	142.3
	C6	d	1	5.268	4.273	41.8	35.7	−149.9

[a]The geometrical descriptors as applied for charged nitrogen–aromatic interactions for the quinuclidine antagonists are defined as follows:[29] θ is the angle C(N1+)-N1...x (centroid), φ is the angle between the normal of the plane of the phenyl ring and the elongation of the vector from N1 to x. C(N1+) indicates the carbon atom adjacent to N1+. The additional dihedral angle C2-N1-C(N1+)...x is given to reconstruct the position of the phenyl ring centroid in space. Note that the orientation of the phenyl ring is not fully determined by the parameters tabulated.
[b]The type of interaction geometry is given in accordance with the preferential geometries given by Verdonk et al.[29]

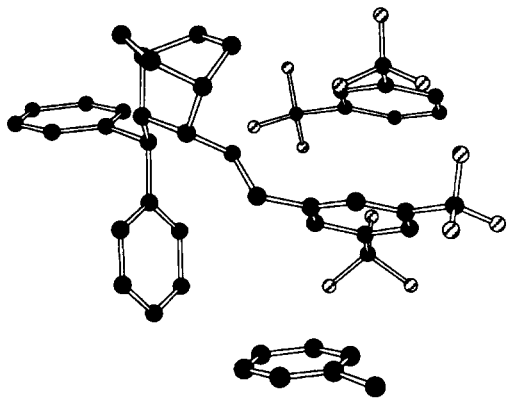

Figure 7. Parallel stacking of the benzylether phenyl ring of L-709,210 (**3**) by two neighbouring phenyl rings. In case of the nearby disubstituted phenyl ring (top), the stacking is mutually accomplished by the trifluoromethyl groups.

In contrast to N1, the pharmacophoric centre N2(O2) is seldomly involved in interactions in the crystal structures of the quinuclidine antagonists; it forms a charge-assisted hydrogen bond with a mesylate anion in structure **1b** and geometrically non-ideal intramolecular hydrogen bonds with the 2-methoxy group of x2 in structures **1a** and **1b** (Fig. 3). The N2(O2) atom of the other quinuclidine structures and the 2-methoxy oxygen atoms in **1a**, **1b** and **2** are not involved in any specific intermolecular interactions.

In structure **3** the disubstituted benzylether phenyl ring x2 is involved in an internal edge-to-face aromatic stack with x1 (Fig. 3). The x2 ring is at the same time positioned parallel (stacked) in between two phenyl groups of neighbouring molecules (Fig. 7). One of these phenyl groups is a 3,5-disubstituted phenyl ring of which the parallel 'stacking' geometry is accomplished by the trifluoromethyl groups attached to both phenyl rings; these groups are located directly above the other ring centroid. No specific interactions of the benzylamino phenyl group x2 in structures of **1a**, **1b** and **2** have been observed.

The benzhydryl groups of CP-96,345 in both crystal structures **1a** and **1b**, form symmetric dimers with the benzhydryl group of neighbouring molecules which are related to the first one by inversion (Figs 8a and b, respectively). In structure **1a** this geometry is stabilized by two edge-to-face aromatic stacks and in **1b** by one face-to-face and two edge-to-face aromatic stacking interactions. Additionally, in structure **1a** the benzhydryl group of the neutral quinuclidine coordinates a phenyl ring in a cooperative fashion (Fig. 8c). These interaction geometries might reflect the possible interactions between the benzhydryl group of **1–3** and the aromatic side-chains of His-197, Phe-268 and Tyr-272 in the human NK_1 receptor.[3] The benzhydryl groups of compounds **2** and **3** only coordinate, by hydrophobic interactions, a methoxy methyl group and the hydrophobic side of a symmetry related quinuclidine ring, respectively, similar to the interaction geometry in Figure 8(c).

Piperidine antagonists

In two out of three piperidine antagonist structures, CP-99,994 (**4**) and CP-210,053 (**5**), both N1 and N2 are protonated, resulting in complete surrounding of their scaffold parts by hydrogen bond acceptor groups (i.e. either chloride anions or, in one case, a water molecule (**5**)). The positions of these groups are similar (designated A, B, C and D) in the two structures and are shown in Figure 9 and indicated in Table 5. The chloride anion in position C is, in contrast to the other hydrogen bond acceptor groups, coordinated by two C–H...Cl^- interactions. In the crystal structure of compound **4** two phenyl rings are partially located within the 5 Å coordination sphere around N1, close to C6 and can probably be regarded as being involved in charged nitrogen–aromatic interactions, even if no strict geometrical criteria can be applied; the N1-centroid distances are 5.24 and 5.47 Å. In the neutral piperidine antagonist **6**, no specific interactions for N1 and N2 were observed.

A major difference in the intermolecular interactions of the doubly protonated piperidines **4** and **5** is observed in the interactions of their aromatic rings. The phenyl rings in the crystal structure conformation of CP-99,994

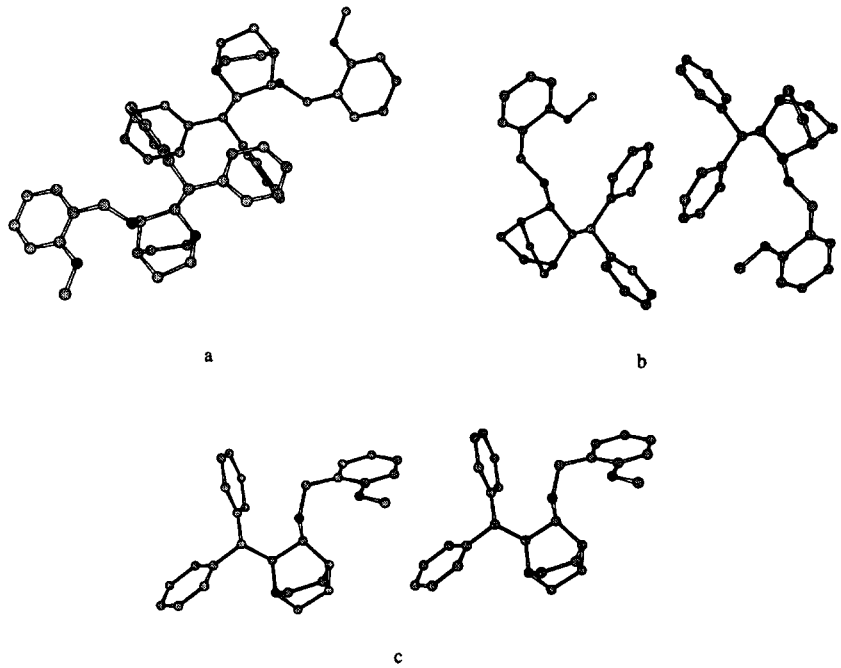

Figure 8. Aromatic–aromatic interaction geometries of the benzhydryl group of CP-96,345 with surrounding phenyl rings. (a) CP-96,345 free base (**1a**), (b) CP-96,345 dimesylate salt (**1b**), and (c) Additional hydrophobic coordination of a phenyl ring by the benzhydryl group of **1a**.

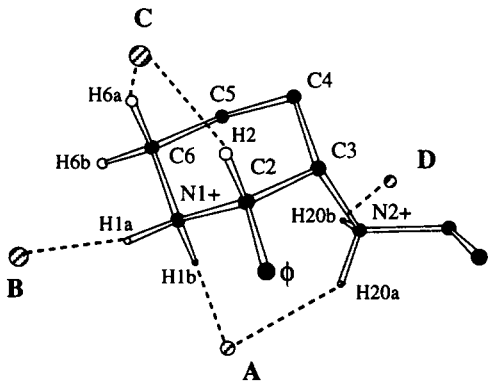

Figure 9. Common hydrogen bond/C–H...X contact acceptor group positions for piperidine NK_1 antagonists. The structure of CP-99,994 (**4**) serves as illustration.

(**4**) are involved in an internal face-to-face aromatic stack, which is stabilized by an intramolecular hydrogen bond between nitrogen N2 and the 2-methoxy group. In addition, both phenyl rings x1 and x2 are involved in an intermolecular edge-to-face aromatic stack (Fig. 10a). In contrast, the phenyl rings of CP-210,053 (**5**), which are involved in an internal edge-to-face stack, are each involved in *three* edge-to-face aromatic stacks with surrounding phenyl rings (Fig. 10b). A threefold edge-to-face aromatic stacking situation is also observed for phenyl ring x2 of the neutral piperidine antagonist **6**, whereas phenyl ring x1 is involved in one edge-to-face aromatic stack (data not shown).

Molecular dynamics simulations on the crystal structure conformations of the conformationally constrained piperidine antagonists **5** and **6** (data not shown) revealed that the N2–H and N2 lone-pair directions are greatly restricted and these compounds might therefore be used in determining the bioactive conformation of the piperidine antagonists. In addition to the crystal structure conformations of **4**, **5** and **6** models were constructed for the solution structure of **5** in $CDCl_3$ as determined by NMR[23] and the N2-inverted configuration of **6**. These five conformations are probably all important energetically accessible conformations and all correspond to staggered conformations around C3–N2 (Table 6, first data column). Upon superposition of the piperidine rings it was noted that there are three regions in space where functional groups interacting with N2 can be located. This is shown in Figure 11. Two of these regions are exemplified by the chloride anion positions A and D in structures **4** and **5**. The third region is indicated by, for example, the N2 (axial) lone pair in the solution conformation of **5** (Table 6 and Fig. 11).

L-Tryptophan benzyl ester antagonists

In the crystal structures of the L-tryptophan benzyl ester analogues **7** and **8** only few heteroatoms are involved in hydrogen bonds, perhaps because of the low number of hydrogen bond donors in the molecules. Comparison of the crystal structure conformations of **7** and the conformationally constrained analogue **8** (Fig. 4) on the one hand suggests that the crystal structure conformation of **7** is not the bioactive conformation: the distance between the centroids of the aromatic rings x1 and x2 in **7** is more than twice the distance in the structure of **8.** On the other hand, the distance between the x1 and x2 aromatic rings in the crystal structure of **7** (i.e. 8.15 Å) corresponds quite well with the x1′–x2 distances in the crystal structures of **1b–3**, which range

Table 5. Common hydrogen bond/C–H...X contact acceptor groups surrounding piperidine antagonists **4** and **5**[a]

				Position A			
No.	**Donor**	**Acceptor**[b]	**D...Ac (Å)**	**C2-N1...Ac (°)**	**C3-N2...Ac (°)**	**C3-C2-N1-Ac (°)**	**C2-C3-N2-Ac (°)**
4	N1-H1b	chloride Cl (2)	3.104(5)	110.4	–	61.8	–
	N2-H20a	chloride Cl (2)	3.261(5)	–	110.3	–	38.5
5	N1-H1b	chloride Cl (1)	3.126(7)	111.4	–	54.9	–
	N2-H20a	chloride Cl (1)	3.161(6)	–	113.3	–	38.0

			Position B		
No.	**Donor**	**Acceptor**	**N1...Ac (Å)**	**C2-N1...Ac (°)**	**C3-C2-N1-Ac (°)**
4	N1-H1a	chloride Cl (1)′	3.063(5)	114.2	−168.9
5	N1-H1a	water O (26)	2.762(10)	93.5	−164.9

			Position C			
No.	**Donor**	**Acceptor**	**N1...Ac (Å)**	**N1-C2...Ac (°)**	**N1-C6...Ac (°)**	**C3-C2-N1-Ac (°)**
4	C2-H2	chloride Cl (2)′	4.131(5)	96.9	81.0	−119.8
5	C6-H6a	chloride Cl (2)′	3.787(8)	83.8	88.5	−116.3

			Position D		
No.	**Donor**	**Acceptor**	**N2...Ac (Å)**	**C3-N2...Ac (°)**	**C2-C3-N2-Ac (°)**
4	N2-H20b	chloride Cl (1)″	3.174(4)	115.8	129.8
5	N2-H20b	chloride Cl (2)″	3.054(7)	119.3	149.7

[a]The table has been constructed in such a way that reconstruction of the hydrogen bond acceptor positions relative to the antagonist structures is possible.
[b]Acceptor atoms are labelled in accordance with the names in the original publication. Symmetry related atoms are indicated by a prime or double prime.

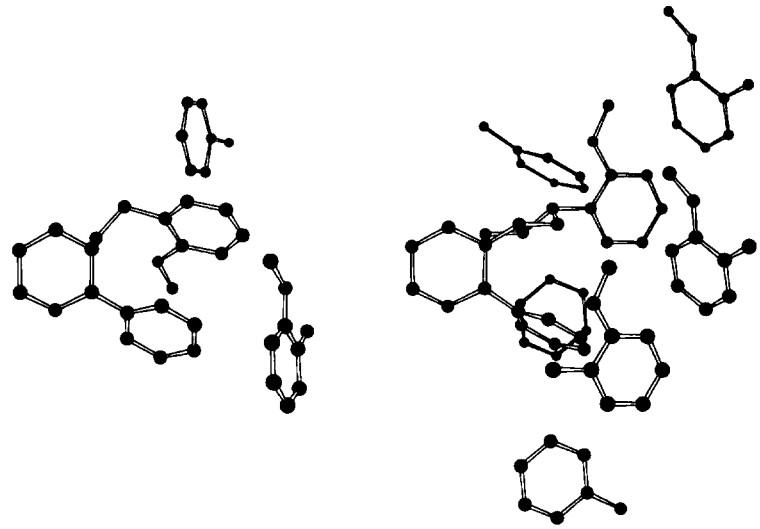

a b

Figure 10. Edge-to-face aromatic–aromatic interaction geometries for the phenyl and benzylamino groups in the crystal structures of the doubly protonated piperidine antagonists. (a) CP-99,994 (**4**) and (b) CP-210,053 (**5**).

from 8.38 Å in **3** to 8.76 Å in **1b**. The indole ring of **7** might therefore also be considered able to occupy the same region as the x1′ group of the quinuclidine antagonists **1–3**, when bound to the NK_1 receptor. Anyhow, both in structures **7** and **8** the 3,5-disubstituted phenyl rings (x2) are involved in intermolecular edge-to-face aromatic stacks as has been reported previously.[11,26] In structure **8** this 'stacking' involves the rotationally disordered trifluoromethyl groups.

Pyrido[3,4-*b*]pyridine carboxamide antagonist

No hydrogen bonds have been observed in the crystal structure of **9**. It seems, however, that the lack of hydrogen bond donors in the crystal is compensated for by short C–H...O contacts with, for example, O2 and O3 (Fig. 4). The pyrido[3,4-*b*]pyridine rings of two symmetry related (in this case mirror image conformations) molecules are stacked in a perfect (anti)parallel manner. In addition, the aromatic rings x1 and x1′, which topologically resemble a 'frozen' benzhydryl group, cooperatively coordinate a trifluoromethyl group.

Superposition of quinuclidine and piperidine antagonists

Desai et al.[16] postulated the pharmacophoric dihedral angle x1–C2–C3–N2(O2) as a descriptor of the struc-

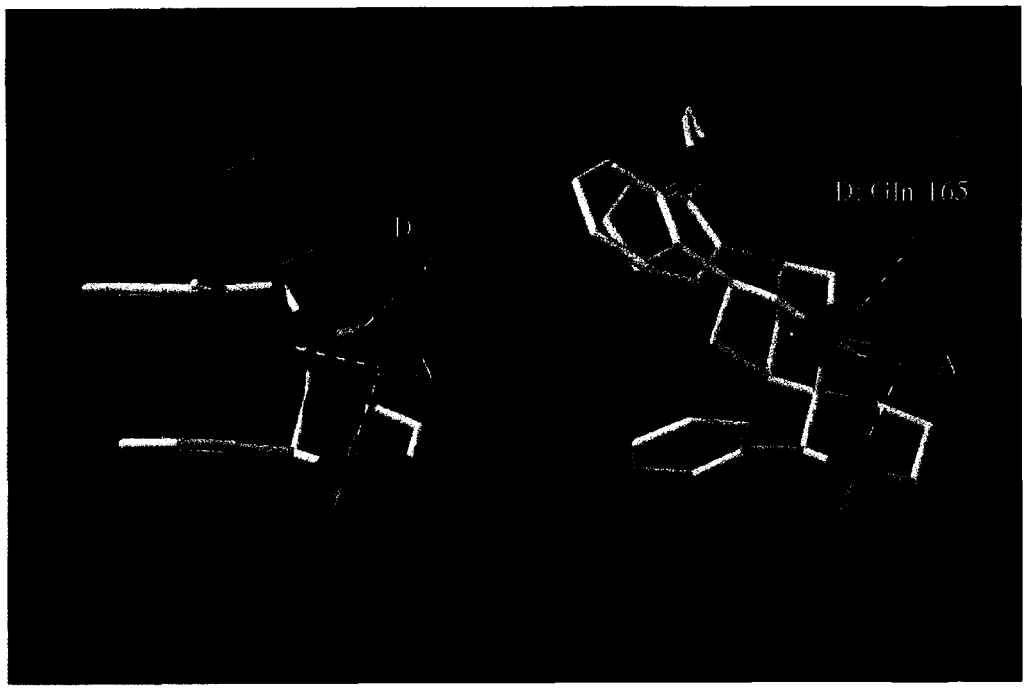

Figure 11. Regions available to groups interacting with N2 in the piperidine antagonists **4**, **5**, and **6**. Structures have been superimposed based on their piperidine rings. The structures of CP-99,994 (**4**) and CP-210,053 (**5**) are shown in white on the left and right, respectively. Structure **6** is given in orange, the modelled solution conformation of CP-210,053 (**5**) is given in yellow. The N2-inverted configuration of **6** is not shown. Chloride anions are shown in green, lone pairs on N2 are shown in magenta. Hydrogen bond acceptor positions are labelled in accordance with Figure 9.

Table 6. Staggered conformations around C3–N2 and interaction sites for N2 for crystal structure and calculated conformations of the piperidine antagonists[a]

No.	Conformation	C2–C3–N2–C (°)	C2–C3–N2–A (°)	C2–C3–N2–D (°)	C2–C3–N2–lp (°)
4	crystal structure	−135.3	38.5	129.8	–
5	crystal structure	−85.2	38.0	147.7	–
	solution (calculated)	−170.0	40.8	–	−45.6
6	crystal structure	−100.1	(22.5)[b]	150.2 or 164.0[c]	–
	N2-inverted (calculated)	156.3	(28.5)[b]	–	−86.0

[a]Atom labelling as given in Figure 9, lp denotes a lone pair.
[b]In these structures position A is occupied by a carbon atom.
[c]The values are determined to anion position D of crystal structures **4** and **5**, respectively.

tural similarity of quinuclidine and piperidine antagonists. To investigate whether this structural similarity is reflected in the intermolecular interactions in the crystal structures, the crystal structure conformations of the quinuclidines **1b**, **2** and **3** were superimposed on the crystal structure conformation of CP-99,994 (**4**) based on a least-squares fit of the corresponding atom pairs x1, C2, C3 and N2(O2). The resulting RMSd values were 0.405, 0.429 and 0.422 Å, respectively. As a typical example, the resulting superposition of CP-96,345 (**1b**) with CP-99,994 (**4**) is depicted in Figure 12. The respective N2 and x1 positions match fairly well, while the N1 positions are clearly distinct. Also, the chloride anion in position C that is common for the piperidine antagonists **4** and **5** was positioned at or nearby the anions at position II of the quinuclidine antagonists. In contrast, the piperidine anion position B is located close to the x1′ centroid of the benzhydryl group of the quinuclidines.

One of the two aromatic rings that can probably be considered to be involved in charged nitrogen–aromatic interactions with the positively charged head group of the piperidine ring of CP-99,994 (**4**) (vide infra) is in close proximity with the positions of both phenyl ring *b* in structure **2** and phenyl ring *d* in structure **3** that are depicted in Figure 6; the intercentroid distances in the superpositions are 2.9 and 2.2 Å, respectively.

In the exemplified case (Fig. 12) of the superposition of CP-96,345 (**1b**) and CP-99,994 (**4**), which are both doubly protonated, two additional anion positions are found at similar sites in space: positions A and D. The mesylate anion in position D is bonded by C–H...O interactions.

Discussion

Crystal structures of nine non-peptide tachykinin NK_1 antagonists have been analysed for the intermolecular

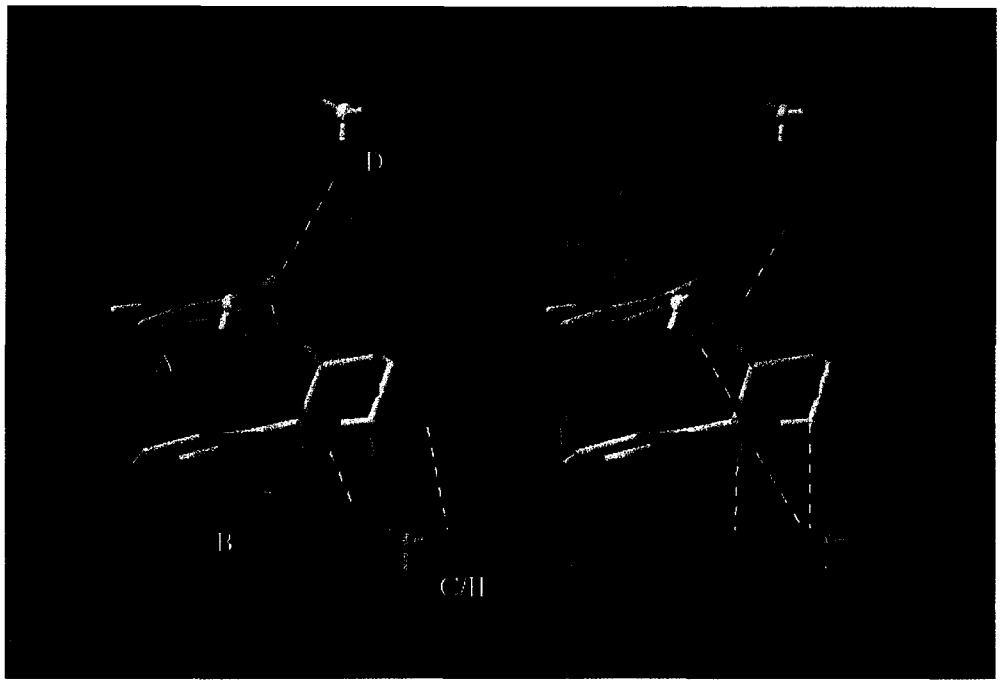

Figure 12. Stereoview of the superposition of the crystal structure conformations of CP-99,994 (**4**) and CP-96,345 (**1b**) based on x1, C2, C3, and N2, RMSd = 0.405 Å. CP-99,994 (**4**) is given in white, CP-96,345 (**1b**) is given in greenblue. Hydrogen bond acceptor positions are labelled in accordance with Figures 5 and 9. Dashed lines indicate hydrogen bonds or C–H...X interactions in **1b** (left) and **4** (right). Chloride anions are shown in green. The mesylate methyl groups have been omitted for clarity.

interactions of their pharmacophoric groups with neighbouring molecules in the crystal. Several interaction geometries have been identified, which are shown to be consistent with both structure–activity relationships and reported receptor interactions for the compounds analysed. A schematic representation of reported ligand–receptor interactions combined with our results for the quinuclidine and piperidine antagonists **1–6** is shown in Figure 13. The interactions encountered in the crystal structures are charge-assisted hydrogen bonds (salt-bridges), C–H...X interactions (X being O, chloride, or iodide), charged nitrogen–aromatic interactions, aromatic–aromatic interactions and hydrophobic interactions.

The quinuclidine antagonists reveal two common hydrogen bond acceptor sites, whenever N1 is positively charged (Fig. 5). Structure–activity studies show that the N1 nitrogen is likely to be positively charged in the active site,[14,27] either by protonation or alkylation as in compound **2**. The rigidity of the quinuclidine framework ensures that no major differences exist between the quinuclidine ring conformation in the crystal structure and in the bioactive state. The same is therefore true for the hydrogen bond acceptor sites. Since the common hydrogen bond acceptor (anion) sites occur both with single-atom anions as well as with the more complex mesylate anions, it stresses the importance of these interactions for a quinuclidine ring containing a positively charged nitrogen. Although the general importance of these hydrogen bond acceptor sites is yet to be confirmed (e.g. by crystal structure statistics) it is likely that these interaction sites are

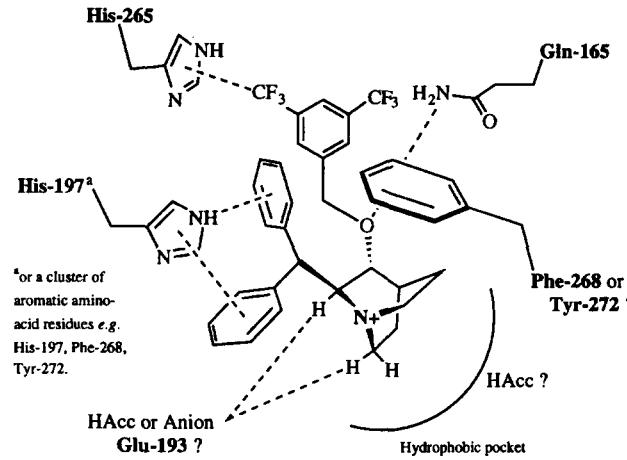

Figure 13. Schematic representation of reported ligand–receptor interactions combined with our results for the quinuclidine and piperidine antagonists **1–6**. 'HAcc' stands for a hydrogen bond acceptor group in the NK_1 receptor. The dashed lines between His-265 and the 3,5-disubstituted phenyl ring and between the centroid of the imidazole ring of His-197 and one of the benzhydryl phenyl rings indicate reported interactions[8,31,34] without inferring the exact nature of the interaction.

relevant candidates for hydrogen bond acceptor groups in the NK_1 receptor. These are indicated by 'HAcc' in Figure 13. The only anionic residue that is a candidate for occupying one of these hydrogen bond acceptor sites in the quinuclidine binding site in the human NK_1 receptor is Glu-193 that is reported to perform an indirect role in antagonist binding,[30] however. It should be noted that electroneutrality in the binding of a positively charged quinuclidine antagonist to the

receptor can also be realized if a free anion would be involved in binding.

Aromatic amino acid residues (including histidines) play an important role in the non-peptide antagonist binding site of the NK_1 receptor.[3] Each of the charged nitrogen–aromatic interaction sites around the protonated quinuclidine ring can therefore be occupied by aromatic amino acid residues in binding to the NK_1 receptor (indicated as a putative hydrophobic pocket in Fig. 13). The presence of these aromatic rings is in agreement with the hydrophobic character of the other ring structures that can replace the quinuclidine ring as a scaffold in NK_1 antagonists.[5] The preferred presence of a hydrogen bond acceptor group (anion position I, Fig. 5) close to these aromatic rings might perhaps additionally be tested in NK_1 antagonist design. One of the aromatic interaction sites (position *c* in Fig. 6 and tentatively indicated as Phe-268 or Tyr-272 in Fig. 13) is especially interesting, because of a cooperative effect of charged nitrogen–aromatic and multiple C–H...π interactions with the quinuclidine and benzhydryl groups, respectively. This interaction site might therefore be specific for the quinuclidine antagonists.

The benzhydryl group of the quinuclidine antagonists is thought to be bound by His-197 of the human NK_1 receptor via amino–aromatic interactions[31] (Fig. 13) or by a cluster of aromatic amino acid residues (His-197, Phe-268 and Tyr-272).[3] Possible interaction geometries for interactions of a benzhydryl group with a cluster of aromatic rings have been suggested by the aromatic stacking geometries in the two crystal structures of CP-96,345 (**1a** and **1b**) studied, as can be seen in Figure 8. Although these interaction geometries only present energetical and geometrical possibilities, they might be used in making binding site models of the human NK_1 receptor.

CP-99,994 (**4**) has been developed based on CP-96,345 (**1**). The inner phenyl ring of the benzhydryl group of CP-96,345 (**1**) with respect to the benzylamino nitrogen was thought to be mimicked by the C2 phenyl ring (x1) in CP-99,994 (**4**). The rationale for the correspondence in NK_1 affinity of both compounds was given by Desai et al.[16] in terms of the dihedral angle x1–C2–C3–N2, which is similar ((+)-*synclinal*) for the quinuclidine and the piperidine antagonists in the crystal structures and in molecular mechanics calculations.[16] A superposition of the crystal structure conformations of quinuclidine and piperidine antagonists based on the elements x1, C2, C3, and N2/O2 resulted in a mismatch of N1, but in corresponding positions for N2 and x1 and hydrogen bond acceptor groups (anions) in C and II (Fig. 12). Also, a corresponding position for aromatic rings involved in charged nitrogen–aromatic interactions in two quinuclidine crystal structures (**2** and **3**) and CP-99,994 (**4**) was observed. The scaffold parts of the quinuclidine and piperidine antagonists thus show similar interactions with their environment (i.e. hydrogen bond acceptor position C/II; Figs 5 and 9) and a charged nitrogen–aromatic interaction. For the diprotonated quinuclidine **1b** additional hydrogen bond acceptor groups match in space with the diprotonated antagonists **4** and **5**. Although the N1 monoprotonated rather than the diprotonated state of the quinuclidine and piperidine antagonists is probably the bioactive state, this resemblance points to a common chemical behaviour of quinuclidine and piperidine antagonists towards their environment. It supports the common binding site[32] that is located for CP-96,345 (**1**) and CP-99,994 (**4**).

In the crystal structures of the quinuclidine antagonists **1** and **2** and piperidine antagonists **4–6**, the 2-methoxy groups are not involved in any specific intermolecular interaction. Yet, internal hydrogen bonds between the 2-methoxy oxygen and the benzylamino nitrogen N2 are present in structures **1a**, **1b** and **4**. It is believed that such an internal hydrogen bond is not required for binding to the NK_1 receptor, via for instance, proper positioning of the phenyl ring x2; the benzylamino nitrogen N2 that would then act as a hydrogen bond donor can be replaced by an oxygen atom that can only act as a hydrogen bond acceptor[12] (e.g. compound L-709,210 (**3**)). Instead, the 2-methoxy substituent in the benzylamino group and the trifluoromethyl substituents in the benzylether group are considered to be required for optimizing interactions with the human NK_1 receptor.

Amino acid residue Gln-165 in the human NK_1 receptor is probably involved as a hydrogen bond donor for N2 and O2 in binding the quinclidine and piperidine antagonists (Fig. 13).[33] Three possible sites for interactions with N2 have been located, determined with the aid of conformationally constrained analogues **5** and **6**. One position (Fig. 11) can be excluded (position A of the piperidine anions) because high affinity binding to the receptor is not lost when this position is not available for the receptor, as in antagonist **6**. Another position is shielded from the receptor by the x1 phenyl ring of the antagonists and is therefore an unlikely candidate interaction site. **The only likely position available to groups interacting with N2 corresponds to chloride position D of the piperidines (Fig. 11)**. This chloride position can then probably be considered as the approximate position of the hydrogen bond donor group in the human NK_1 receptor: the amide side-chain of Gln-165. This site is geometrically described by standard hydrogen bond criteria and the dihedral angle C2–C3–N2–D, which should be in the range of 130–164° (Table 6). In this argument we consider the crystal structure conformations of CP-99,994 (**4**) and **5** also energetically accessible when N2 is not protonated. Consequently, the crystal structure conformation of **5** is likely to be close to its bioactive conformation, given its relative rigidity in the molecular dynamics simulations and the inability of hydrogen bond formation between N2 and D in the solution structure of **5** (Fig. 11).

A histidine residue in the human NK_1 receptor, His-265, is reported to be involved in binding the phenyl ring of the benzylamino and benzylether group of quinuclidine antagonists (Fig. 13).[34] The crystal structures of the piperidine antagonists provide aromatic–

aromatic interaction geometries for this phenyl ring. They are, however, related to the specific benzylamino conformation encountered. A non-parallel intramolecular geometry of the two phenyl rings resulted in more aromatic–aromatic interactions for the benzylamino phenyl rings in the crystal structures of CP-210,053 (**5**) and (**6**) versus CP-99,994 (**4**) (Fig. 10). This might suggest that a non-parallel orientation of phenyl rings x1 and x2 in both quinuclidine and piperidine antagonists has more possibilities for interactions in the human NK_1 receptor, which would create a favourable situation when aromatic–aromatic interactions (e.g. with His-265) are of importance. In addition, the trifluoromethyl groups of the 3,5-disubstituted phenyl rings of benzylether quinuclidine **3** and L-tryptophan benzyl ester analogue **8** seem to mediate both the parallel and perpendicular stacking geometries of these phenyl rings in the two structures, respectively. This might be part of the role of the trifluoromethyl substituents in the interaction of the 3,5-disubstituted phenyl rings with His-265.[8,34]

From the class of the L-tryptophan benzyl ester antagonists a potent 3,5-bis(trifluoromethyl) analogue[35] of compound **7**, namely L-732,138 was reported to bind at more or less the same binding site on the human NK_1 receptor as the benzylether quinuclidine antagonist **3**, despite their structural differences.[8] This similarity in binding is not reflected in the few intermolecular interactions observed in the crystal structures of compounds **7** and **8**, with respect to compound **3**. In structures **7** and **8** the limited functionality available in the crystal environment compared to that in a protein might be due to this. To a lesser extent this is of course also true for **3**. Additionally, it might be argued that the crystal structure conformation of **7** is, by reference to its constrained analogue **8**, probably not the bioactive one. Alternatively, the indole ring of **7** can be considered to occupy the x1′ position of the quinuclidine antagonists **1–3** (vide infra), when bound to the NK_1 receptor, rather than the position of phenyl ring x1.

Compound **9** can topologically be regarded as a hybrid of the L-tryptophan benzyl ester antagonists **7** and **8** (especially the carbonyl groups) and the benzylether quinuclidine **3** (3,5-disubstituted benzyl group and 'locked-in' benzhydryl group). Also, a comparison of the intersection volumes of antagonist **9** and CP-99,994 (**4**) in two modelled conformations has suggested that these compounds are able to occupy similar regions in space.[17] In that superposition the carbonyl oxygen O2 of **9** was located at the N2 position of CP-99,994 (**4**). In the crystal structure of **9** no interactions substantiating any similarity with CP-99,994 (**4**) have been observed.

In analyzing intermolecular interactions in individual crystal structures, we have to be aware that they might be heavily biased due to the limited choice of functional groups in the crystal. Interaction geometries may be found only because no better alternative exists. Only interaction geometries that are in agreement with results from crystal structure statistics or high-quality calculations can therefore be validly considered. Additionally, for all structures the likely difference in crystal structure conformation of flexible parts of a molecule to its bioactive conformation has to be taken into account. To understand the mechanism of recognition and binding of ligands to their receptor whenever an experimentally determined structure of a protein–ligand complex is absent, it is not sufficient to study interactions between ligands and their environment by molecular biological techniques or by analyzing intermolecular interactions in the crystal structures of the ligands. In addition to these experimental results, theoretical conformational analysis of the antagonists in relation to calculated properties indicative of interactions with the receptor environment, and the construction of binding site models is highly desirable for a more thorough understanding.

Experimental

Evaluation of interactions

Hydrogen bonds were identified as such when the (potential) donor–hydrogen–acceptor angle (D–H...A) was larger than 100.0°, the hydrogen–acceptor distance was below the sum of their van der Waals radii minus 0.12 Å and the donor–acceptor distance was lower than the sum of their van der Waals radii augmented by 0.5 Å.[18] Additionally, when these criteria are applied to locate C–H...X interactions (X=N, O, Cl, or I usually as anions) the donor C–H group should be adjacent to a positively charged nitrogen and the hydrogen–acceptor distance should be below (or equal to) the sum of the van der Waals radii minus 0.2 Å.[20]

Charged nitrogen–aromatic interaction geometries were evaluated according to the parameters defined by Verdonk et al.[29] for all aromatic rings with at least one aromatic ring carbon atom within 5 Å of any carbon atom bonded to a positively charged nitrogen.

Aromatic–aromatic interactions were classified as such when the centroids of two aromatic rings were not more than 6 Å apart, their interplane angle deviated from being perfectly parallel or perpendicular by no more than 30° and the smallest of the two angles between the normal of one of the rings with the vector between the centroids of the two rings was maximally 30°.[18,36]

Tables 3, 4 and 5 have been constructed in such a way that reconstruction of the positions of the hydrogen bond acceptor groups and aromatic rings relative to the quinuclidine and piperidine rings of the antagonists is possible. In addition, files of the crystal structure conformations with all surrounding groups within 5 Å of the central ligand are available from the authors on request.

Model building

Molecular dynamics simulations on initial crude models of the NMR and N2 inverted conformation (configura-

tion) of compounds **5** and **6**, respectively, were performed to obtain energetically reasonable conformations. The geometry of the initial models was first optimized to a final energy gradient 0.001 kcal mol^{-1} $Å^{-1}$, using conjugate gradients. Then a 25 ps molecular dynamics simulation was performed at 298 K, following 5 ps equilibration. Calculations were performed with the CVFF force field in DISCOVER 2.96 (INSIGHTII 2.3.5)[37] using a dielectric constant of 1. The simulations were performed on the neutral species. The final conformations were then subjected to semi-empirical geometry optimizations performed using the AM1 Hamiltonian[24] in the MOPAC93 program.[25] Explicit definition of the geometry optimization via the eigenvector following routine, controlled by the PRECISE keyword (i.e. EF PRECISE SCFCRT=1.D-6 GNORM=0.01) was employed. MOPAC calculations were prepared and finally analysed using SYBYL 6.2.[13]

The initial N2 inverted model of **6** was directly subjected to semi-empirical geometry optimization; molecular dynamics simulations starting with the N2 inverted model of **6** returned the crystal structure configuration every time.

Acknowledgements

We thank Harry R. Howard for the crystal data on CP-211,754, and Richard T. Lewis and Richard G. Ball for the crystal data of L-732,244 and L-709,210. Access to the PLATON program and helpful discussions on it by Ton Spek are gratefully acknowledged.

References

1. Pascard, C. *Acta Cryst.* **1995**, *D51*, 407.

2. Glusker, J. P. *Acta Cryst.* **1995**, *D51*, 418.

3. Gether, U.; Lowe, III J. A.; Schwartz, T. W. *Biochem. Soc. Trans.* **1995**, *23*, 96.

4. Regoli, D.; Boudon, A.; Fauchere, J. L. *Pharmacol. Rev.* **1994**, *46*, 551.

5. Desai, M. C. *Exp. Opin. Ther. Patents* **1994**, *4*, 315.

6. Ward, P.; Armour, D. R.; Bays, D. E.; Evans, B.; Giblin, G. M. P.; Heron, N.; Hubbard, T.; Liang, K.; Middlemiss D.; Mordaunt, J.; Naylor, A.; Pegg, N. A.; Vinader, M. V.; Watson, S. P.; Bountra, C.; Evans, D. C. *J. Med. Chem.* **1995**, *38*, 4985.

7. Desai, M. C.; Lefkowitz, S. L.; Bryce, D. K.; McLean, S. *Bioorg. Med. Chem. Lett.* **1994**, *4*, 1865.

8. Cascieri, M. A.; Macleod, A. M.; Underwood, D.; Shiao, L. L.; Ber, E.; Sadowski, S.; Yu, H.; Merchant, K. J.; Swain, C. J.; Strader, C. D.; Fong, T. M. *J. Biol. Chem.* **1994**, *269*, 6587.

9. Allen, F. H., Davies, J. E.; Galloy, J. J.; Johnson, O.; Kennard, O.; Macrae, C. F.; Mitchell, E. M.; Mitchell, G. F.; Smith, J. M.; Watson, D. G. *J. Chem. Inf. Comput. Sci.* **1991**, *31*, 187.

10. Howard, H. R.; Shenk, K. D.; Coffman, K. C.; Bryce, D. K.; Crawford, R. T.; McLean, S. A. *Bioorg. Med. Chem. Lett.* **1995**, *5*, 111.

11. Lewis, R. T.; MacLeod, A. M.; Merchant, K. J.; Kelleher, F.; Sanderson, I.; Herbert, R. H.; Cascieri, M. A.; Sadowski, S; Ball, R. G.; Hoogsteen, K. *J. Med. Chem.* **1995**, *38*, 923.

12. Swain, C. J.; Seward, E. M.; Cascieri, M. A.; Fong, T. M.; Herbert, R.; MacIntyre, D. E.; Merchant, K. J.; Owen, S. N.; Owens, A. P.; Sabin, V.; Teall, M.; Van Niel, M. B.; Williams, B. J.; Sadowski, S.; Strader, C. D.; Ball, R. G.; Baker, R. *J. Med. Chem.* **1995**, *38*, 4793.

13. Tripos Associates, 1699 S. Hanley Road, St Louis, MI 63144-2913, U.S.A., 1995.

14. Lowe, III J. A.; Drozda, S. E.; Snider, R. M.; Longo, K. P.; Zorn, S. H.; Morrone, J.; Jackson, E. R.; McLean, S.; Bryce, D. K.; Bordner, J.; Nagahisa, A.; Kanai, Y.; Suga, O.; Tsuchiya, M. *J. Med. Chem.* **1992**, *35*, 2591.

15. Snider, R. M.; Constatine, J. W.; Lowe, III J. A.; Longo, K. P.; Lebel, W. S.; Woody, H. A.; Drozda, S. E.; Desai, M. C.; Vinick, F. J.; Spencer, R. W.; Hess, H. J. *Science* **1991**, *251*, 435.

16. Desai, M. C.; Lefkowitz, S. L.; Thadeio, P. F.; Longo, K. P.; Snider, R. M. *J. Med. Chem.* **1992**, *35*, 4911.

17. Natsugari, H.; Ikeura, Y.; Kiyota, Y.; Ishichi, Y.; Ishimaru, T.; Saga, O.; Shirafuji, H.; Tanaka, T.; Kamo, I.; Doi, T.; Otsuka, M. *J. Med. Chem.* **1995**, *38*, 3106.

18. Spek, A. L. *Acta Cryst.* **1990**, *A46*, C34.

19. Burley, S. K.; Petsko, G. A. *Adv. Prot. Chem.* **1988**, *39*, 125.

20. Taylor, R.; Kennard, O. *J. Am. Chem. Soc.* **1982**, *104*, 5063.

21. Allen, F. H. *Acta Cryst.* **1986**, *B42*, 521.

22. Bernstein, J.; Davis, R. E.; Shimoni, L.; Chang, N. L. *Angew. Chem. Int. Ed. Engl.* **1995**, *34*, 1555.

23. Desai, M. C.; Vincent, L. A.; Rizzi, J. P. *J. Med. Chem.* **1994**, *37*, 4263.

24. Dewar, M. J. S.; Zoebisch, E. G.; Healy, E. F.; Stewart, J. P. *J. Am. Chem. Soc.* **1985**, *107*, 3902.

25. Stewart, J. P. *J. Comput.-Aided Mol. Design* **1990**, *4*, 1.

26. Macleod, A. M.; Merchant, K. J.; Brookfield, F.; Kelleher, F.; Stevenson, G.; Owens, A. P.; Swain, C. J.; Cascieri, M. A.; Sadowski, S.; Ber, E.; Strader, C. D.; MacIntyre, D. E.; Metzger, J. M.; Ball, R. G.; Baker, R. *J. Med. Chem.* **1994**, *37*, 1269.

27. Lowe, III J. A.; Drozda, S. E.; McLean, S.; Crawford, R. T.; Bryce, D. K.; Bordner, J. *Bioorg. Med. Chem. Lett.* **1994**, *4*, 1153.

28. Dougherty, D. A. *Science* **1996**, *271*, 163.

29. Verdonk, M. L.; Boks, G. J.; Kooijman, H.; Kanters, J.; Kroon, J. *J. Comput.-Aided Mol. Design* **1993**, *7*, 173.

30. Gether, U.; Nilsson, L.; Lowe, III J. A.; Schwartz, T. W. *J. Biol. Chem.* **1994**, *269*, 23959.

31. Fong, T. M.; Cascieri, M. A.; Yu, H.; Bansal, A.; Swain, C.; Strader, C. D. *Nature* **1993**, *362*, 350.

32. Pradier, L.; Habert-Ortoli, E.; Emile, L.; Le Guern, J.; Loquet, I.; Bock, M. D.; Clot, J.; Mercken, L.; Fardin, V.; Garret, C.; Mayaux, J. F. *Mol. Pharmacol.* **1995**, *47*, 314.

33. Fong, T. M.; Yu, H.; Cascieri, M. A.; Underwood, D.; Swain, C. J.; Strader, C. D. *J. Biol. Chem.* **1994**, *269*, 14957.

34. Fong, T. M.; Yu, H.; Cascieri, M. A.; Underwood, D.; Swain, C. J.; Strader, C. D. *J. Biol. Chem.* **1994**, *269*, 2728.

35. Macleod, A. M.; Merchant, K. J.; Cascieri, M. A.; Sadowski, S.; Ber, E.; Swain, C. J.; Baker, R. *J. Med. Chem.* **1993**, *36*, 2044.

36. Hunter, C. A.; Sanders, J. K. M. *J. Am. Chem. Soc.* **1990**, *112*, 5525.

37. Biosym Technologies, 9685 Scranton Road, San Diego, CA 92121-2777, U.S.A., 1995.

(*Received in U.S.A.* 27 *August* 1996; *accepted* 29 *October* 1996)